Plotkin SA. 2001. Rubella eradication. Vaccine 19:3311–3319.

Rajasundari TA, Sundaresan P, Vijayalakshmi P, Brown DW, Jin L. 2008. Laboratory confirmation of congenital rubella syndrome in infants: An eye hospital based investigation. J Med Virol 80:536–546.

Reef SE, Frey TK, Theall K, Abernathy E, Burnett C, Icenogle J, McCauley MM, Wharton M. 2002. The changing epidemiology of rubella in the 1990s: On the verge of elimination and new challenges for control and prevention. JAMA 287:464–472.

Terry GM, Ho-Terry L, Londesborough P, Rees KR. 1988. Localization of the rubella E1 epitopes. Arch Virol 98:189–197.

Tran DN, Vu MP, Ha MT, Giang TPL, Komase K, Mizuguchi M, Ushijima H. 2011. Viral molecular characterization of the first congenital rubella syndrome case in Vietnam. Clin Lab 57:397–401.

Valinotto LE, Viegas M, Acevedo ME, Barrero PR, Mistchenko AS. 2009. Phylogenetic analysis of rubella viruses isolated in 2008 outbreak in Argentina. J Clin Virol 46:286–289.

Vauloup-Fellous C, Hübschen JM, Abernathy ES, Icenogle J, Gaidot N, Dubreuil P, Parent-du-Châtelet I, Grangeot-Keros L, Muller CP. 2010. Phylogenetic analysis of rubella viruses involved in congenital rubella infections in France between 1995 and 2009. J Clin Microbiol 48:2530–2535.

World Health Organization. 2005. Standardization of the nomenclature for genetic characteristics of wild-type rubella viruses. Wkly Epidemiol Rec 80:126–132.

World Health Organization. 2006. Global distribution of measles and rubella genotypes-update. Wkly Epidemiol Rec 81:474–479.

World Health Organization. 2007. Update of standard nomenclature for wild-type rubella viruses, 2007. Wkly Epidemiol Rec 24:216–222.

World Health Organization Western Pacific Region. 2010. Special topic: Accelerating rubella control. Measles-Rubella Bull 4:8–9.

Yan H, Yagyu F, Okitsu S, Nishio O, Ushijima H. 2003. Detection of norovirus (GI, GII), sapovirus and astrovirus in fecal samples using reverse transcription single-round multiplex PCR. J Virol Methods 114:37–44.

Zhu Z, Abernathy E, Cui A, Zhang Y, Zhou S, Zhang Z, Wang C, Wang T, Ling H, Zhao C, Chen Y, He J, Sun L, Chen X, Tang J, Feng D, Wang Y, Ba Z, Fan L, Chen H, Pan Z, Zhan J, Chen H, Zhou S, Zheng L, Gao H, Liang Y, Dai D, Icenogle J, Xu W. 2010. Rubella virus genotypes in the People's Republic of China between 1979 and 2007: A shift in endemic viruses during the 2001 Rubella Epidemic. J Clin Microbiol 48:1775–1781.

Jpn. J. Infect. Dis., 65, 268-270, 2012

Laboratory and Epidemiology Communications

Imported Cases of Measles in Niigata, Japan in 2011

Kanako Watanabe[1]*, Kaori Watanabe[1], Takashi Tazawa[1], Miyako Kon[1], Tsutomu Tamura[1], and Katsuhiro Komase[2]

[1]*Virology Section, Niigata Prefectural Institute of Public Health and Environmental Sciences, Niigata 950-2144; and*
[2]*Department of Virology III, National Institute of Infectious Diseases, Tokyo 208-0011, Japan*

Communicated by Makoto Takeda

(Accepted February 24, 2012)

In Japan, the measles surveillance system was changed in January 2008, from sentinel surveillance of children and adults to nationwide case-based reporting on the basis of experience from a large measles outbreak, and to achieve measles elimination by 2012, according to an agreement reached among Western Pacific Region member states. All medical practitioners were required to report every clinical or laboratory-confirmed measles case to a local public health center (1).

According to the new surveillance-reporting system, we have performed laboratory diagnoses of suspected measles cases in Niigata Prefecture. From 2008 to 2011, a total of 42 clinical specimens (throat swab, blood, and/or urine samples) were collected from 18 individuals with suspected measles. These collected samples were tested by measles virus (MV)-specific reverse transcription-nested polymerase chain reaction (2). We detected 4 hemagglutinin (*H*) and 3 nucleoprotein (*N*) genes of MV from 3 patients who had returned from abroad. This report summarizes these 3 imported cases of measles in Niigata, Japan in 2011.

Patient 1 was a 7-month-old Malaysian boy who had stayed in Malaysia for about 5 months after the 2011 Great East Japan Earthquake disaster with his brother apart from their mother. Their mother, who resided in Niigata, had visited Malaysia on August 15 and brought back her children to Japan on September 1. On August 29, Patient 1 developed a fever (over 39°C), which was followed by a rash on September 2. In fact, in mid-August, his brother had been hospitalized with the same symptoms in Malaysia. Throat swab, blood, and urine samples of Patient 1 were collected on September 8: *H* and *N* genes of MV were detected only from the throat swab.

Patient 2 was an 11-month-old boy who resided in Niigata. He had not been immunized against measles. Patient 3 was his mother, a 33-year-old Japanese woman who had been immunized against measles once. They had visited New Zealand for 10 days (from September 17 to 26). On October 4, Patient 2 developed a fever (38.8°C), which was followed by a rash on October 8. His throat swab, blood, and urine samples were collected on October 13; *H* and *N* genes of MV were detected from the throat swab, and the *H* gene alone was detected from the urine sample. On October 12, 8 days after onset of the illness in Patient 2, Patient 3 developed a fever (38.9°C), which was followed by a rash on October 13. Her throat swab and blood samples were harvested on October 12; *H* and *N* genes of MV were detected only from the throat swab.

Patients 1 and 2 were reported to a local public health center as measles cases and Patient 3 was classified as having modified measles, due to her measles vaccination history and atypical symptoms, such as a shorter period of rash.

For genetic analysis, partial nucleotide sequences of the *N* gene (456 bp) of the MV strains were determined by the direct sequencing method (2). These sequences were analyzed phylogenetically using Molecular Evolutionary Genetics Analysis (MEGA) software (version 5). Evolutionary distances were estimated using the maximum composite likelihood method and the phylogenetic tree was constructed using the neighbor-joining (NJ) method. The reliability of the phylogenetic tree was estimated by 1,000 bootstrap replications.

The 3 sequences from Patients 1, 2, and 3 were designated MVs/Niigata.JPN/38.11, MVs/Niigata.JPN/42.11/1, and MVs/Niigata.JPN/42.11/2, respectively, according to the World Health Organization nomenclature, and deposited in the DNA Data Bank of Japan with the accession numbers AB675481, AB678710, and AB678711, respectively.

Phylogenetic analysis revealed that MVs/Niigata.JPN/38.11 belonged to genotype D9, represented by MVs/Victoria.AUS/12.99, and MVs/Niigata.JPN/42.11/1 and MVs/Niigata.JPN/42.11/2, which were identical, belonged to genotype D4, represented by MVi/Montreal.CAN/89 (Fig. 1). The sequence homologies between MVs/Victoria.AUS/12.99 and MVs/Niigata.JPN/38.11, and between MVs/KLumpur.MYS/21.11 and MVs/Niigata.JPN/38.11 were 97.8% and 99.3%, respectively. Similarly, those between MVi/Montreal.CAN/89 and MVs/Niigata.JPN/42.11/1, and between MVs/Auckland.NZL/23.11 and MVs/Niigata.JPN/42.11/1 were 97.5% and 100%, respectively. The D9 genotype of MV was reported from Australia, Hong Kong (China), Japan, Malaysia, New Zealand, Philippines, Republic of Korea, and Singapore in 2011. On the other hand, the D4 genotype of MV was reported from Australia, Japan, New Zealand, and Singapore and caused outbreaks in Europe, Africa, and the

*Corresponding author: Mailing address: Virology Section, Niigata Prefectural Institute of Public Health and Environmental Sciences, 314-1 Sowa, Nishi-ku, Niigata 950-2144, Japan. Tel: +81 (25) 263-9414, Fax: +81 (25) 263-9410, E-mail: watanabe.kanako@pref.niigata.lg.jp

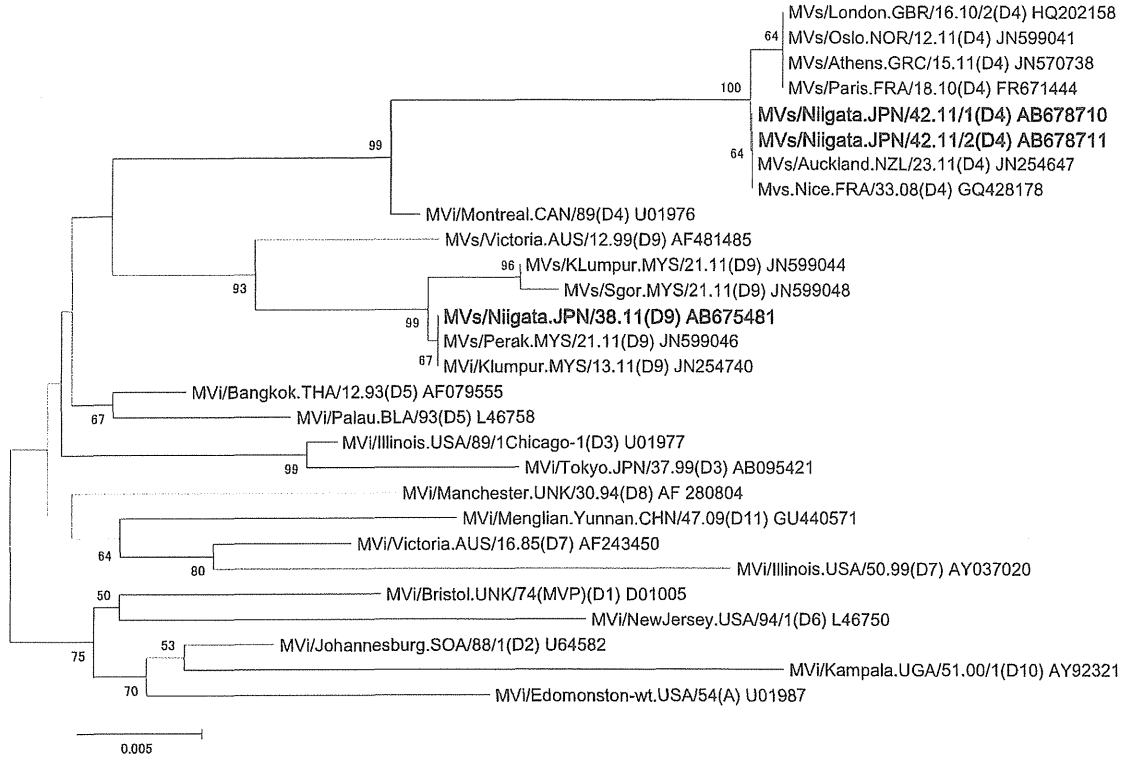

Fig. 1. Phylogenetic tree based on the nucleoprotein gene sequences (456 bp) of genotype A and D reference strains of the measles virus. The evolutionary distance was calculated using the maximum composite likelihood method, and the tree was plotted using the neighbor-joining method. Numbers at each branch indicate the bootstrap values of the clusters supported by that branch. The scale indicates 0.5% nucleotide differences. DDBJ/EMBL/GenBank accession numbers are given in parentheses. The present strains are represented in bold type.

Americas in 2011 (3–5). From our laboratory data along with epidemiological information, these 3 patients were considered infected with MVs circulating in the countries they had each visited, and finally confirmed as cases of imported measles or import-related measles.

In the United States, in addition to vaccinating infants aged 6–11 months, it is recommended that people who have insufficient measles immunity be administered the measles vaccine prior to travel abroad (6). People should recognize the risk of exposure to measles during a stay abroad, regardless of whether a stay is long or short, and receive the measles vaccine as needed in advance, in order to protect themselves as well as to avoid bringing back measles into Japan. Fortunately, no outbreak has been reported around the cases described here.

Only 2 measles cases in 2010 and 3 imported or import-related cases in 2011 were reported in Niigata Prefecture, which has a population of 2.4 million. Consequently, Niigata Prefecture has achieved the measles elimination target (under 1 case per million population, excluding imported cases) (7). Moreover, the measles vaccination rate in the 2010 fiscal year was 97%, 97%, 95%, and 91% for the 1st (at 1 year of age), 2nd (at 5–6 years), 3rd (at 12–13 years), and 4th (at 17–18 years) vaccinations (8), respectively, and 95% of the population over 2 years of age were seropositive for measles in 2010 (9). Therefore, measles is no longer considered to be endemically transmitted in Niigata Prefecture. In addition, some of the other prefectures in Japan have also achieved the measles elimination target (7) and endemic measles transmission might have ceased in these prefectures. However, resurgence of measles transmission by MV from abroad or from endemic prefectures is easily conceivable, because MV is highly contagious. Therefore, maintenance of high-level immunity against measles and an appropriate surveillance system are required to prevent the resurgence of measles in Niigata.

Conflict of interest None to declare.

REFERENCES

1. Sunagawa, T., Shimada T, Ueno-Yamamoto, K., et al. (2008): Progress toward measles elimination—Japan, 1999–2008. Morbid. Mortal. Wkly. Rep., 57, 1049–1052.
2. National Institute of Infectious Diseases (2008): Manual for the Diagnosis of Measles. 2nd version. National Institute of Infectious Diseases, Tokyo, Japan. Online at 〈http://www.nih.go.jp/niid/reference/measle-manual-2.pdf〉 (in Japanese).
3. World Health Organization Western Pacific Region (2011): Measles-Rubella Bulletin, 5, December 1–6.
4. World Health Organization (2011): Measles Outbreaks in Europe. Global Alert and Response. Online at 〈http://www.who.int/csr/don/2011_04_21/en/〉.
5. World Health Organization (2011): Measles Outbreaks: Regions of the Americas, Europe and Africa. Global Alert and Response. Online at 〈http://www.who.int/csr/don/2011_10_07/en/〉.
6. Centers for Disease Control and Prevention (2012): Yellow Book-Traveler's Health Chapter 3, Infectious Diseases related to travel, Measles (Rubeola). Online at 〈http://wwwnc.cdc.gov/travel/yellowbook/2012/chapter-3-infectious-diseases-related-to-travel/measles-rubeola.htm〉.

7. National Institute of Infectious Diseases and Tuberculosis and Infectious Diseases Control Division, Ministry of Health, Labour and Welfare (2011): Measles in Japan, 2010. Infect. Agent Surveillance Rep., 32, 31'-32'.
8. Ministry of Health, Labour and Welfare (2011): Measles Vaccination Rate by Prefecture in the 2010 Fiscal Year in Japan. Online at 〈http://www.mhlw.go.jp/bunya/kenkou/kekkaku-kansenshou21/dl/110331a.pdf〉 (in Japanese).
9. Niigata Prefectural Institute of Public Health and Environmental Sciences (2011): Measles particle agglutination antibody acquisition rate by age group. Annu. Rep. Niigata Pref. Inst. Public Health Environ. Sci., 26, 38 (in Japanese).

Jpn. J. Infect. Dis., 65, 94-97, 2012

Laboratory and Epidemiology Communications

An Isolated Incidence of Rubella Outbreak at a Workplace in Hokkaido, Japan

Masahiro Miyoshi[1]*, Rika Komagome[1], Hideki Nagano[1], Kenichi Takahashi[1], Hiroshi Koba[2], Yumiko Kaneko[2], Yasuko Watanabe[2], Fumiaki Suzuki[2], Takashi Hiroshima[2], Ichiro Aida[3], Sayaka Kitamura[4], Naosuke Saji[5], Ryo Yamaguchi[5], and Motohiko Okano[1]

[1]*Center for Infectious Diseases Control, Hokkaido Institute of Public Health, Sapporo 060-0819;*
[2]*Hokkaido Government Shiribeshi General Subprefectural Bureau, Kutchan 044-8588;*
[3]*Hokkaido Government Tokachi General Subprefectural Bureau, Obihiro 080-8588;*
[4]*Hokkaido Government Ishikari General Subprefectural Bureau, Sapporo 060-8558; and*
[5]*Department of Health and Welfare, Hokkaido Government, Sapporo 060-8558, Japan*

Communicated by Makoto Takeda

(Accepted December 19, 2011)

Rubella is an acute and contagious disease that is mainly characterized by fever, rash, and cervical lymphadenopathy (1). Under the Law Concerning Prevention of Infectious Diseases and Medical Care for Patients with Infectious Diseases (the Infectious Diseases Control Law) in Japan, rubella has been classified as a category V infectious disease and requires mandatory reporting instead of sentinel reporting since January 1, 2008 (2). Here, we report an isolated rubella outbreak that occurred among adults in Hokkaido.

On May 14, 2011, some workers reported fever and rash (Table 1). Initially, we tested for the presence of measles antibodies as a part of the process of eliminating measles in Japan. We obtained leukocyte (serum in the case of some patients), throat swab, and/or urine samples from 9 patients (Table 2) and analyzed these samples using enzyme immunoassay (EIA) for measles-

*Corresponding author: Mailing address: Center for Infectious Diseases Control, Hokkaido Institute of Public Health, North 19 West 12, Kita-ku, Sapporo 060-0819, Japan. Tel: +81-11-747-2764, Fax: +81-11-747-2757, E-mail: miyo@iph.pref.hokkaido.jp

Table 1. Epidemiological information of the patients

Patient no.	Age	Date of arrival in Hokkaido	Accommodation	Date of onset[1)]	Date of onset (rash)	Vaccination status
1	20s	2011/4/20	A	5/9	5/13	Unknown
2	30s	4/11	B	5/11	5/13	Unknown
3	50s	—	Own home	5/12	5/18	Unvaccinated
4	40s	4/20	C	5/13	5/13	Unvaccinated
5	20s	—	Own home	5/13	5/14	Unknown
6	40s	4/20	C	5/14	5/15	Unvaccinated
7	30s	4/20	F	5/15	5/15	Unvaccinated
8	40s	3/28	E	5/15	5/16	Unknown
9	30s	4/21	C	5/15	5/18	Unknown
10	30s	4/20	B	5/16	5/17	Unknown
11	40s	4/24	D	5/16	5/17	Unknown
12	30s	4/17	G	5/19	Unclear	Unknown
13	40s	Resident of Hokkaido	H	5/20	5/23	Unknown
14	40s	Resident of Hokkaido	I	5/21	5/21	Unknown
15	30s	4/29	J	5/23	5/23	Unknown
16	30s	4/18	C	5/28	6/2	Once
17	40s	—	Own home	6/1	6/2	Unknown

1): Date indicates the day of onset including two or more of the following symptoms: fever (15), lymphadenopathy (3), headache (4), cough (3), sore throat (5), catarrh (5), malaise (5), arthralgia (4), inertia (1), fundus oculi pain (1), sputum (1), and diarrhea (1). Number in patenthesis indicates the number of cases having symptoms.

Table 2. Specific tests for rubella virus in this outbreak

Patient no.*	Days after onset**	Rubella virus-specific antibodies			RT-PCR		
		Specimen	IgM index value[1)]	IgG index value[2)]	Specimen	NS	E1
1	8	Serum	0.44	0.15	Serum	−	−
3	7	Plasma	0.64	1.07	PBMC	−	−
					Ts	+	+
					U	+	+
7	2	Serum	2.16	0.16	Serum	−	−
8	2	Serum	0.02	0.13	PBMC	+	+
					Ts	+	+
					U	+	+
9	4	Plasma	0.14	0.27	PBMC	+	+
					Ts	+	+
					U	−	−
10	4	Plasma	2.36	0.31	PBMC	−	−
					Ts	+	+
					U	+	−
11	1	Plasma	0.25	0.09	PBMC	+	−
					Ts	+	+
					U	+	+
12	1	Plasma	0.07	0.12	PBMC	−	−
					Ts	+	−
					U	−	−
13	4	Plasma	0.2	0.06	PBMC	−	ND
					Ts	+	+
					U	+	−

* and **: Case number and the date of onset are corresponded with Table 1.
1): IgM index value $\geqq$1.21 is defined as positive.
2): IgG index value $\geqq$1.0 is defined as positive.
PBMC, peripheral blood mononuclear cells; Ts, throat swab; U, urine; −, negative; +, positive; ND, not done.

specific immunoglobulin (IgM) and tests for detecting the genomes of measles virus. However, the results of these tests were negative. Rubella virus may cause the formation of rashes similar to those observed in measles (1). For this reason, we analyzed the collected samples using an EIA kit (Denka Seiken Co., Tokyo, Japan) with rubella virus-specific IgM and IgG antibodies and/or evaluated the presence of both nonstructural

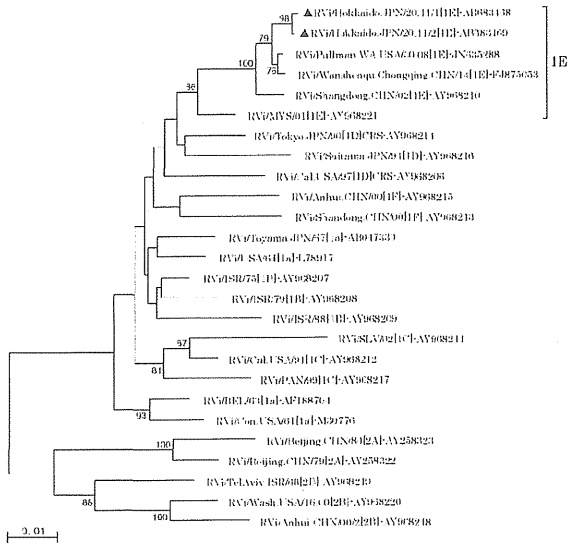

Fig. 1. Phylogenetic tree based on the 739-nucleotide region of E1 gene of rubella virus. Bootstrap values above 75 are shown, and the samples obtained in this outbreak are marked with black triangles.

protein (NS) and envelope protein 1 (E1) genes of rubella virus using reverse-transcriptase polymerase chain reaction (RT-PCR) (3) (Mori Y, personal communication). As shown in Table 2, the rubella virus-specific IgM antibodies were present in 2 patients (Nos. 7 and 10), while the rubella virus-specific IgG antibody was present in only 1 patient (No. 3). In addition, 6 patients (Nos. 3, 8–11, and 13) were positive for both NS and E1 genes and 1 patient (No. 12) was positive only for the NS gene. Phylogenetic analyses using the neighbor-joining method were performed by direct sequencing of 739 nucleotides of E1 gene, which corresponded to the minimum acceptable window defined by the World Health Organization (4). Nucleotide sequences determined in this study have been submitted to the DNA Data Bank of Japan (GenBank accession nos. AB683468 and AB683469). Two groups of the sequence (RVi/Hokkaido.JPN/20.11/1 and RVi/Hokkaido. JPN/20.11/2) were detected, and the genotypes of both the groups were highly homologous to that of the 1E strains of rubella virus. There was only one synonymous substitution between them (Fig. 1). The genotype 1E genome was also reported in an outbreak that occurred in Niigata Prefecture in the same year (5).

From the clinical manifestations and laboratory findings, total of 17 patients (men; age range, 20s–50s) were diagnosed as rubella (Tables 1 and 2). All the patients had no history of travel to foreign countries. Five of the patients were local residents, and the remaining were from areas outside Hokkaido. Fourteen patients, including 2 local residents, had stayed temporarily at accommodation facilities near the workplace. Three patients (Nos. 1, 4, and 11) had arrived possibly during the incubation period of the disease (12–23 days prior to the onset of infection). The earliest case, patient No. 1, showed onset of symptoms on May 9, after which more patients fell ill on every day from May 11 to 16. Additionally, 11 patients showed the onset of symptoms during May 9–16, and they stayed at 8 different accommodation facilities. Therefore, the epidemiological survey suggests that several patients, including Nos. 1, 4, and 11, were most probably exposed to the rubella virus at around the same time.

A person with rubella can generally shed the virus from 7 days before and after the onset of rash (1). Patient No. 1 was considered as the earliest case because the rashes in this patient were first notified on May 13. Patients (Nos. 1–11) who showed onset of the symptoms until May 16 were considered to be initially infected during similar period. Patients (Nos. 12–17) who showed onset of the symptoms after May 19 were considered to have been secondarily infected. Further, since patient No. 16 (onset of symptoms on May 28) had used the same accommodation facility that was used by patient Nos. 4, 6, and 9 (onset of symptoms on May 13, 14, and 15, respectively), he may have contracted the infection from the workplace or the accommodation facility. During and after this outbreak, no sporadic cases of rubella were reported in Hokkaido.

Only patient No. 16 had a history of rubella vaccination, whereas the other patients were not aware of their vaccination statuses (Table 1). Until the Immunization Law in Japan was amended in 1994, routine immunization for rubella virus was performed only for female students of junior high school from 1977; between 1989 and 1993, the measles-mumps-rubella vaccine was optionally administered to infants aged 12–72 months. Therefore, adult men aged 30–40 years are presently considered to be highly susceptible to rubella (6). The present study supports this claim since the rubella virus outbreak, which showed that the rubella virus-specific IgG antibodies were absent in many male patients during the early phase of the infection.

Seven patients were negative for rubella virus-specific IgM antibodies, and clinical specimens from 5 of them were collected on the same day as the onset of rash. During the early phase of the infection, it is difficult to diagnose the disease on the basis of serological findings alone (7). The symptoms of rubella are often mild or subclinical (1). However, rubella virus infection in pregnant women may cause congenital rubella syndrome (CRS) (1,8,9). The occurrence of CRS is most likely to coincide with a rubella epidemic (10). Thus, improved immunization and effective surveillance systems are critical for preventing infection and eliminating rubella.

This article appeared in the Infectious Agents Surveillance Report (IASR), vol. 32, p. 254–255, 2011 in Japanese.

Acknowledgments The authors are grateful to the staff of the regional hospital for collecting the samples and providing the epidemiological data. The authors also thank Dr. Yoshio Mori of the National Institute of Infectious Diseases of Japan for providing the technical advice.

Conflict of interest None to declare.

REFERENCES

1. Centers for Disease Control and Prevention (2001): Control and prevention of rubella: evaluation and management of suspected outbreaks, rubella in pregnant women, and surveillance for con-

genital rubella syndrome. Morbid. Mortal. Wkly. Rep., 50 (RR-50), 1–23.
2. Ministry of Health, Labour and Welfare (2008): Operation of the laws revising a part of the Law Concerning Prevention of Infectious Diseases and Medical Care for Patients with Infectious Diseases and the Quarantine Law. Online at 〈http://www.mhlw.go.jp/bunya/kenkou/kekkaku-kansenshou04/16.html〉 (in Japanese).
3. Suzuki, J., Goto, H., Komase, K., et al. (2010): Rubella virus as a possible etiological agent of Fuchs heterochromic iridocyclitis. Graefes. Arch. Clin. Exp. Ophthalmol., 248, 1487–1491.
4. World Health Organization (2005): Standardization of the nomenclature for genetic characteristics of wild-type rubella viruses. Wkly. Epidemiol. Rec., 80, 126–132.
5. Watanabe, K., Tazawa, T., Watanabe, K., et al. (2011): Rubella outbreak in a workplace, May 2011-Niigata. Infect. Agents Surveillance Rep., 32, 252–254 (in Japanese).
6. Taya, K., Sato, H., Arai, S., et al. (2011): Immunization history and rubella seroprevalence among the healthy population in Japan in the year 2010—national epidemiological surveillance of vaccine preventable diseases [updated August 2011]. Infect. Agents Surveillance Rep., 32, 263–266 (in Japanese).
7. Abernathy, E., Cabezas, C., Sun, H., et al. (2009): Confirmation of rubella within 4 days of rash onset: comparison of rubella virus RNA detection in oral fluid with immunoglobulin M detection in serum or oral fluid. J. Clin. Microbiol., 47, 182–188.
8. Ushida, M., Okada, T. and Kato, S. (2000): Case of congenital rubella syndrome transmitted from reinfected mothers. Infect. Agents Surveillance Rep., 21, 6–7 (in Japanese).
9. Miller, E., Cradock-Watson, J.E. and Pollock, T.M. (1982): Consequences of confirmed maternal rubella at successive stages of pregnancy. Lancet, 320, 781–784.
10. Terada, K. (2003): Rubella and congenital rubella syndrome in Japan: epidemiological problems. Jpn. J. Infect. Dis., 56, 81–87.

Jpn. J. Infect. Dis., 65, 367-369, 2012

Laboratory and Epidemiology Communications

An Outbreak of Exanthematous Disease due to Coxsackievirus A9 in a Nursery in Yamagata, Japan, from February to March 2012

Yoko Aoki[1], Akiko Abe[2], Tatsuya Ikeda[1], Chieko Abiko[1], Katsumi Mizuta[1]*, Ichiro Yamaguchi[3], and Tadayuki Ahiko[1]

[1]*Department of Microbiology, Yamagata Prefectural Institute of Public Health, Yamagata 990-0031;*
[2]*Department of Pediatrics, Shinoda Hospital, Yamagata 990-0045; and*
[3]*Murayama Public Health Center, Yamagata 990-0031, Japan*

Communicated by Makoto Takeda

(Accepted June 14, 2012)

Between late February and early March of 2012, an outbreak of exanthematous disease was identified in a nursery in Yamagata, Japan. Of the 3 infants and 47 children enrolled at the nursery, 27 (11 boys and 16 girls) children aged between 4 months and 6 years (median, 1 year and 10 months) presented with fever and exanthema. These children were clinically diagnosed with viral exanthema. In addition, one of the children enrolled at the nursery had 2 siblings (aged 4 months and 1 year) who did not attend the nursery, but were diagnosed with the same disease.

To investigate the causative agents of the viral outbreak, we collected throat swabs and serum or whole blood specimens from a total of 11 patients. We isolated the virus and subsequently performed reverse transcription (RT)-PCR analysis (Table 1). For virus isolation, we used the microplate method, which included 6 previously described cell lines: human embryonic lung fibroblast (HEF), human laryngeal carcinoma (HEp-2), African green monkey kidney (Vero E6), Madin Darby Canine Kidney (MDCK), rhabdomyosarcoma (RD-18S), and green monkey kidney (GMK) cell lines (1). After centrifugation of the specimens at 3000 rpm for 20 min, 75 μl of the supernatant was inoculated directly onto 2 wells of each cell line. The remainder of each

*Corresponding author: Mailing address: Department of Microbiology, Yamagata Prefectural Institute of Public Health, Tokamachi 1-6-6, Yamagata, Yamagata 990-0031, Japan. Tel: +81-23-627-1373, Fax: +81-23-641-7486, E-mail: mizutak@pref.yamagata.jp

Table 1. Clinical information and results of laboraotry examination for the patients with exanthematous diseases at a nursery

Patient no.	Age	Clinical sign	Laboratory examination			Status of measles-rubella vaccine
			Specimen	Virus isolation	RT-PCR	
1	3Y	fever, exanthema	throat swab	CVA9	EV(CVA9)	Received
2	2Y	fever, exanthema	throat swab	CVA9	EV(CVA9)	Received
3	1Y	fever, exanthema	throat swab, serum	CVA9 Not done	EV(CVA9), rubella Negative	Not received
4	1Y	fever, exanthema	serum	Not done	Negative	Received
5	1Y	fever, exanthema	throat swab, whole blood	CVA9 Not done	EV(CVA9) Negative	Received
6	6M	exanthema	throat swab	Negative	rubella	Not received
7	7M	fever, exanthema	throat swab	CVA9	EV(CVA9)	Not received
8[1)]	1Y	fever, exanthema	throat swab	Negative	EV(CVA9)	Not received
9[1)]	1Y	fever, exanthema	throat swab	CVA9	EV(CVA9)	Not received
10[2)]	1Y	fever, exanthema, swelling of lymph nodes	serum, throat swab	Not done CVA9	Negative EV(CVA9)	Received
11[2)]	4M	fever, exanthema	throat swab	CVA9	EV(CVA9)	Not received

[1)]: No. 8 and No. 9 are twins.
[2)]: Although they do not attend the nursery, their older sister goes to the nursery.
Y, year old; M, month old; CVA9, coxsackievirus A9; EV, enterovirus.

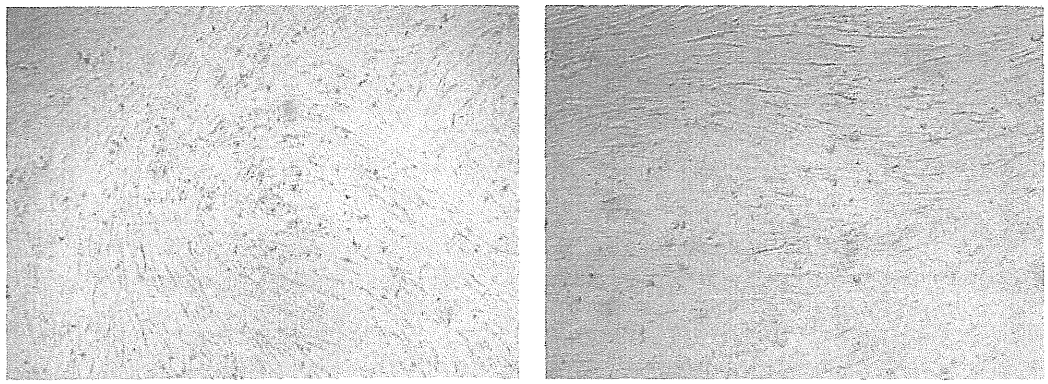

Fig. 1. Cytopathic effect of coxsackievirus A9 virus isolated from Patient no. 1 in HEF cells. Rounding, shrunk, and degenerated cell are observed.

specimen was stored at −80°C. The inoculated plates were centrifuged for 20 min at 2000 rpm, incubated at 33°C in a 5% CO_2 incubator, and assessed for cytopathic effect (CPE) over the course of 14 days; the Vero E6 cell lines were observed for approximately 1 month without media changes to isolate human metapneumoviruses (hMPVs) (1,2). When an enterovirus-like CPE was observed (Fig. 1), we used a neutralization test, RT-PCR, and sequence analysis for identification and validation. Moreover, we tried to amplify the genomes of measles virus, rubella virus, enterovirus, and parvovirus using the following primers: MHL1, MHR1, MHL2, and MHR2 for measles (3); Rub-NSL F3 1F (5′-TCCTTGCGCCGAAGACT-3′), Rub-NSL B3-6 1R (5′-AGAGGGGGTCCACTTGAG-3′), Rub-NSL F2 nestF (5′-CCACTGAGACCGGCTGCGA-3′), and Rub-NSL B2 nestR (5′-GCCTCGGGGAGGAAGAT GAC-3′) for rubella; 9895-forward and 9565-reverse for enterovirus (4) and PVB-1 (5′-CACTATGAAAACT GGGCAATAAAC-3′), PVB-2 (5′-ATTGATTCTCC TGAACTGGTCC-3′), PVB-3 (5′-ATAAACTACAC TTTTGATTTCCCTG-3′), and PBV-4 (5′-TCTCCT GAACTGGTCCCG-3′) for parvovirus.

Hence, we successfully isolated coxsackievirus A9 (CVA9) from 8 patients using the HEF and RD-18S cell lines (Table 1). Additionally, we were able to amplify the enterovirus genome, which was confirmed as CVA9 in 9 patients by sequence analysis (Table 1). The presence of the rubella virus genome was detected in 2 patients who had not received the measles-rubella vaccination. However, we could not confirm an increase in antibody titers against the rubella virus using the hemagglutination inhibition test with paired sera for Patient no. 3, in whom we had isolated CVA9 and detected the rubella virus genome from an identical throat swab specimen. Thus, we concluded that this outbreak of exanthematous diseases was due to infection with CVA9. From our experience, we learned that, although difficult at times, differential diagnosis of viral exanthematous disease is extremely crucial.

Now that the measles elimination project has been progressing in Japan, the differential diagnosis of acute exanthematous diseases is critically important. The rashes associated with viral exanthematous diseases such as measles, rubella, enterovirus, parvovirus, herpes simplex, human herpesvirus 6, and varicella are very similar in appearance; they may be clinically indistinguishable in some cases (5,6). We have actively moni-

tored exanthematous diseases and carried out laboratory and differential diagnoses of measles virus infections in Yamagata to eventually eliminate measles entirely. In 2005, we had reported probable cases of measles, and in 2009, we had confirmed imported cases due to genotype D9 (7,8). Furthermore, even though 6 cases of suspected measles surfaced in Yamagata in 2011, we were able to rule out measles infection in all of these cases; we isolated rhinovirus from 1 patient and detected the rubella virus in 2 other patients (9). As a result, for the first time, we could report no cases of measles virus infections in Yamagata Prefecture in 2011. As predicted in 2005 (7), we observed that as the number of measles cases decreases, the role played by public health laboratories becomes increasingly important, as these are the primary agencies that genotype and monitor the circulation and transmission pathways of measles virus and conduct differential diagnosis of viral exanthematous diseases such as rubella and CVA9.

Acknowledgments We thank the doctors, nurses, and people of Yamagata Prefecture for their assistance and collaboration in the surveillance of viral infectious diseases and Drs. Komase K. and Mori Y. for providing us with the primer sequences for rubella and parvovirus.

This work was supported by grants-in-aid from the Japan Society for Promotion of Science and for Research on Emerging and Re-emerging Infectious Diseases from the Ministry of Health, Labour and Welfare of Japan.

Conflict of interest None to declare.

REFERENCES

1. Mizuta, K., Abiko, C., Aoki, Y., et al. (2008): Analysis of monthly isolation of respiratory viruses from children by cell culture using a microplate method: a two-year study from 2004 to 2005 in Yamagata, Japan. Jpn. J. Infect. Dis., 61, 196–201.
2. Abiko, C., Mizuta, K., Itagaki, T., et al. (2007): Outbreak of human metapneumovirus detected by Vero E6 cell line in Yamagata, Japan between 2004 and 2005. J. Clin. Microbiol., 45, 1912–1919.
3. Saito, H., Harada, S., Tanaka, K., et al. (1994): Rapid detection and typing method for measles virus using reverse-transcription polymerase chain reaction method. Annu. Rep. Akita Pref. Inst. Public Health, 38, 33–35 (in Japanese).
4. Savolainen, C., Blomqvist, S., Mulders, M.N., et al. (2002): Genetic clustering of all 102 human rhinovirus prototype strains: serotype 87 is close to human enterovirus 70. J. Gen. Virol., 83, 333–340.
5. National Institute of Infectious Diseases and Tuberculosis and Infectious Diseases Control Division, Ministry of Health, Labour and Welfare (2012): Measles in Japan, 2011. Infect. Agents Surveillance Rep., 33, 27'–28'.
6. Modlin, J.F. (2004): Enteroviruses. p. 117–142. *In* A.A. Gershon, P.J. Hotez and S.L. Katz (eds.), Krugman's Infectious Diseases of Children. Mosby, Pennsylvania.
7. Mizuta, K., Abiko, C., Murata, T., et al. (2005): An outbreak of measles virus infection due to a genotype D9 at a junior high school in Yamagata, Japan in 2004. Jpn. J. Infect. Dis., 58, 98–100.
8. Aoki, Y., Mizuta, K., Suto, A., et al. (2009): Importation of the evolving measles virus genotype D9 to Yamagata, Japan from Thailand in 2009. Jpn. J. Infect. Dis., 62, 481–482.
9. Aoki, Y., Ikeda, T., Abiko, C., et al. (2011): Imported rubella virus infections, which were suspected measles cases. Rep. Yamagata Pref. Inst. Public Health, 44, 6–8 (in Japanese).

Protein & Peptide Letters, 2012, *19*, 468-473

Crystallization Strategy for the Glycoprotein-Receptor Complex between Measles Virus Hemagglutinin and its Cellular Receptor SLAM

Takao Hashiguchi[a], Toyoyuki Ose[b,c], Marie Kubota[a], Nobuo Maita[d], Jun Kamishikiryo[b], Katsumi Maenaka[b,c,e,*] and Yusuke Yanagi[a,*]

[a]*Department of Virology, Faculty of Medicine, and* [b]*Research Center for Prevention of Infectious Diseases, Medical Institute of Bioregulation, Kyushu University, Fukuoka 812-8582, Japan.* [c]*Faculty of Pharmaceutical Sciences, Hokkaido University, Kita-12, Nishi-6, Kita-ku, Sapporo 060-0812, Japan.* [d]*Institute for Enzyme Research, University of Tokushima, 3-18-15 Kuramoto-cho, Tokushima 770-8503, Japan.* [e]*Core Research for Evolutional Science and Technology, Japan Science and Technology Agency, 4-1-8, Honcho Kawaguchi, Saitama 332-0012, Japan*

Abstract: Measles virus (MV), one of the most contagious agents, infects immune cells using the signaling lymphocyte activation molecule (SLAM) on the cell surface. A complex of SLAM and the attachment protein, hemagglutinin (MV-H), has remained elusive due to the intrinsic handling difficulty including glycosylation. Furthermore, crystals obtained of this complex are either nondiffracting or poorly-diffracting. To solve this problem, we designed a systematic approach using a combination of the following techniques; (1) a transient expression system in HEK293SGnTI(-) cells, (2) lysine methylation, (3) structure-guided mutagenesis directed at better crystal packing, (4) Endo H treatment, (5) single-chain formation for stable complex, and (6) floating-drop vapor diffusion. Using our approach, the receptor-binding head domain of MV-H covalently fused with SLAM was successfully crystallized and diffraction was improved from 4.5 Å to a final resolution of 3.15 Å. These combinational methods would be useful as crystallization strategies for complexes of glycoproteins and their receptors.

Keywords: crystallization, floating-drop vapor diffusion, glycoprotein, HEK293SGnTI(-) cells, lysine methylation, measles virus hemagglutinin, receptor, SLAM.

INTRODUCTION

Crystal structures of viral glycoprotein-receptor complexes not only enable us to glean essential information for understanding the pathogenesis of diseases but also provide us with scaffolds for drug and vaccine design and templates for biomimetics. However, there exist problematic bottlenecks in protein expression, complex formation, crystallization, cryocooling and data collection, which further hinders protein complexes crystals from reaching sufficient resolution to allow structure determination. However, barriers exist in each step of the crystallization process. Glycoproteins in general express poorly and they exhibit weak binding affinity toward their receptors. Glycoprotein-receptor complex crystals can be very fragile and inadequate cryocooling will often destroy these delicate crystals. In addition, many glycoproteins are heavily glycosylated and these heterogeneous sugar-modified proteins often disfavor crystallization. Here, we utilize the example of MV to address each barrier presented in the crystallization process and to showcase a rational design to improve crystallization.

*Address correspondence to this author at the Faculty of Pharmaceutical Sciences, Hokkaido University, Kita-12, Nishi-6, Kita-ku, Sapporo 060-0812, Japan; Tel: +81-11-706-3970; Fax: +81-11-706-4986; E-mail: kmaenaka-umin@umin.net
Department of Virology, Faculty of Medicine, Kyushu University, Fukuoka 812-8582, Japan; Tel: +81-92-642-6138; Fax: +81-92-642-6140; E-mail: yyanagi@virology.med.kyushu-u.ac.jp

MV is an enveloped, non-segmented, negative-stranded RNA virus that belongs to the *Morbillivirus* genus in the *Paramyxoviridae* family [1]. MV causes 'measles' which is currently responsible for an annual 4 % of deaths worldwide in children younger than 5 years of age [2]. MV infection causes severe immunosuppression, leading to secondary complications among measles patients resulting in high morbidity and mortality [3].

To enter the target cell, the lipid-bilayer enveloped MV must bind to their cellular receptors and induce fusion of the viral envelope with the host cell membrane. MV possesses two envelope glycoproteins, hemagglutinin (MV-H) and fusion (F) protein, which are responsible for receptor binding and membrane fusion, respectively [4]. MV-H binds to the signaling lymphocyte activation molecule (SLAM, also called CD150), which is a member of the immunoglobulin (Ig) superfamily and comprise of the SLAM family including 2B4, CD48, CD84, CD229, CD319, and natural killer, T- and B-cell antigen (NTB-A). SLAM acts as a self ligand and is a membrane glycoprotein that is expressed exclusively on immature thymocytes, activated lymphocytes, macrophages and dendritic cells [5]. In addition, SLAM is reported to be a marker for the most primitive hematopoietic stem cells in mice [6]. Because MV targets immune cells using SLAM as a receptor, it exhibits lymphotropism and immunosuppressive property in hosts [4,7]. Furthermore, MV infects polarized epithelial cells using an as-yet-unknown receptor molecule [8, 9], thereby presumably facilitating transmission via

0929-8665/12 $58.00+.00

aerosol droplets [10,11]. Vaccine strains of MV also use ubiquitously expressed glycoprotein CD46 as an alternate receptor through mutations in MV-H [12]. To date, three measles virus glycoprotein structures have been determined: a receptor-free form (MV-H), a CD46-binding form (MV-H-CD46), and a SLAM-binding form (MV-H-SLAM) [12-15].

Here we report a systematic approach in crystallization using our recently reported structure of the MV-H and its cellular receptor SLAM [14] as an example. In our approach, we utilized an extensive repertoire of techniques to first obtain diffracting crystals and then improve resolution from 7 Å to 3.15Å. This strategy would be useful as a template for developing rational approaches for co-crystallization of glycoproteins and their receptors in general.

EXPRESSION AND PURIFICATION

MV-H is a type II integral membrane glycoprotein that contains an N-terminal cytoplasmic tail, a single transmembrane domain, a membrane-proximal stalk domain and a large C-terminal head domain (Genbank, AB583749) [1,3]. The head domain is responsible for the attachment to its cellular receptors, SLAM, an as-yet-unknown receptor expressed on epithelial cells, and CD46. SLAM is a type I membrane protein comprised of V-set and C2-set Ig-like extracellular domains, a transmembrane domain and a cytoplasmic tail (Genbank, AF257239) [5]. It has been reported that the membrane-distal V-set domain is necessary and alone, is sufficient to function as a receptor [16].

In the present study, the pCA7sec vector was used as an expression vector for all expression constructs [18]. The receptor-binding head domain of MV-H (Asp^{149} to Arg^{617}) and the V-set Ig like domain of human and marmoset SLAM (Met^{1} to Gln^{140}) (hSLAM and maSLAM, respectively) containing C-terminal His^{6} tag were expressed in HEK293-SGnTI(-) cells lacking the N-acetylglucosaminyltransferase I activity, which make N-linked glycans of the proteins restricted and homogeneous (oligomannose, $Man_5GlcNAc_2$) [17]. HEK293SGnTI(-) cells was employed to increase successful crystallization of sugar-modified proteins, whose heterogeneous sugars usually inhibit crystallization. Since the pCA7sec vector contains the SV40 replication origin, the protein expression levels were increased by co-transfection with the plasmid encoding the SV40 large T antigen (pCA7-SV40) [18].

Plasmid vectors were transfected using polyethyleneimine into 90 % confluent HEK293SGnTI(-) cells with the ratio of 1.0 : 1.5 (DNA : polyethyleneimine) in Dulbecco's modified Eagle's medium (DMEM) (MP Biomedicals, Inc.) containing 2 % fetal calf serum (FCS) (Invitrogen). The concentration of FCS was increased to 2 % immediately after mixing the plasmid and polyethyleneimine in DMEM without FCS. The cells were cultured in 15 cm dish (surface area, 177 cm^2). Supernatant containing each soluble protein was collected at 5 days post-transfection. Then, it was mixed with 10 x Ni-NTA column binding buffer to a final concentration of 50 mM NaH_2PO_4 pH 8.0, 150 mM NaCl, and 10 mM imidazole and incubated at 277 K overnight. The mixture was centrifuged at 5,500 *g* at 277 K for 10 minutes and the supernatant was filtrated through 0.22 mm filter. Subsequently, the solution containing the His^{6}-tagged MV-H protein was loaded onto a Ni-NTA column. It was washed with 20 column volumes of wash buffer (50 mM NaH_2PO_4 pH 8.0, 150 mM NaCl, 10 mM imidazole) and then eluted with elution buffer (50 mM NaH_2PO_4 pH 8.0, 150 mM NaCl, 500 mM imidazole). The eluted sample was further purified by size-exclusion chromatography (Superdex 200GL 10/300 (Amersham Biosciences)) equilibrated with the HBS buffer (20 mM HEPES pH7.5 and 100 mM NaCl). The purified proteins were of expected sizes as analyzed by non-reducing SDS-PAGE with Coomassie brilliant blue Fig. (**1**). MV-H (D149-R617) alone on SDS-PAGE gel exhibits a homodimer by forming the intermolecular C154-C154 disulfide bond (construct a in Fig. (**1**)). However, the MV-H-SLAM single-chain constructs expressed in this study (constructs c-i in Fig. (**1**)) comprise MV-H of only from S184 to T607. Therefore, they do not form the intermolecular C154-C154 disulfide bond. Approximately 2 mg of MV-H protein, 0.1 mg of maSLAM-V protein, and 3.0 mg of MV-H-$(GGGS)_n$ linker-maSLAM-V complexes were obtained from thirty three 15 cm dishes of HEK293SGnTI(-) cells (1L medium), respectively

CRYSTALLIZATION AND DATA COLLECTION

Initial crystallization screenings for the 1:1 mixture of the MV-H and SLAM proteins were performed by the sitting drop vapor diffusion techniques with the 96-well high-throughput crystallography plate (Axygen Biosciences, Inc) and the Mosquito® crystallization robot (TTP LabTech Ltd). A comprehensive set of commercially available kits were used; Crystal Screen and Crystal Screen II (Hampton Research), Wizard 1 and Wizard 2 (Emerald Biostructures), and the NeXtal series (The Classics Suite, Protein Complex Suite, MbClass suite, MbClass II Suite, Anions Suite and ComPAS suite) (QUAGEN). However, co-crystallizations of MV-H with hSLAM or maSLAM were unsuccessful. The crystals obtained were either non-diffracting or poorly diffracting. Therefore, we introduced a reductive methylation of lysine to change the characters of the proteins [19]. The purified protein (1.0 mg/ml) was treated with 20 mM dimethylboron and 40 mM HCHO at 4 °C overnight, and then re-purified by size exclusion chromatography with the running buffer (20 mM imidazole pH8.0 and 100 mM NaCl). Native crystals of the complex between MV-H (residues Asp^{149} to Arg^{617}) and maSLAM-V (residues Met^{1} to Gln^{140}) were obtained with Crystal Screen I solution H6 (100 mM MES, pH 6.5, 1.6 M magnesium sulfate). The crystals were obtained only by the sitting drop vapor diffusion method at 293 K from a mixture containing 1:1 ratio (0.2 µl) of protein solution (9.3 mg/ml, in 20 mM imidazole, pH 8.0, 100 mM NaCl) to mother liquor (100 mM MES, pH 6.5, 0.75 M lithium sulfate monohydrate) Fig. (**2A**). The best crystal diffracted anisotropically with the highest resolution limit up to 4.5 Å resolution at beamline BL5A of Photon Factory in KEK (Tsukuba, Japan). The diffraction data were processed with HKL2000 suite [19] and indexed to the space group $P6_322$. The unit cell dimensions are a= 208.1 Å, b=208.1 Å, c=182.1 Å (R_{merge}= 0.078, completeness= 100.0 %) and contains one MV-H-SLAM molecule per asymmetric unit [14]. A reductive methylation of lysine has been used successfully in crystallization of murine hepatitis virus NSP9 and Murray Valley encephalitis virus NS5A [21]. In our case, diffracting

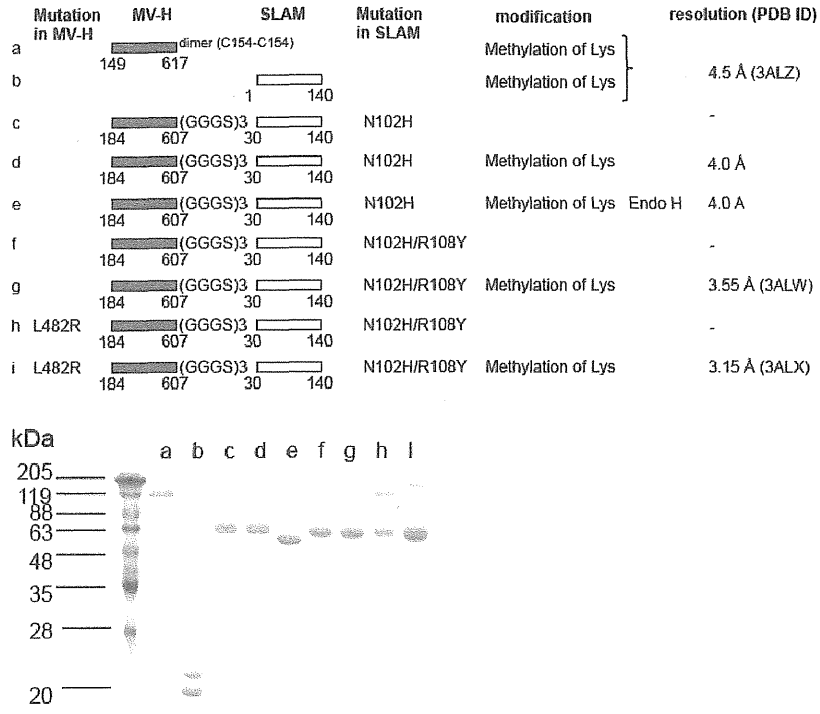

Figure 1. SDS-PAGE (top) and structures (bottom) of MV-H, maSLAM-V and MV-H-maSLAM-V complex proteins examined in this study. Oligomannose-type MV-H, maSLAM-V and MV-H-maSLAM-V complexes expressed in HEK293SGnTI(-) cells under non-reducing condition. **a**. methylated MV-H (residues Asp^{149} to Arg^{617}) protein. **b**. methylated maSLAM-V (residues Met^{1} to Gln^{140}) protein. maSLAM-V shows different molecular weights depending on the patterns of N-linked glycosylation. **c**. MV-H (residues Ser^{184} to Thr^{607})-maSLAM-V (residues Met^{30} to Gln^{140} with N102H substitution) linked by a 12-residue flexible linker $(GGGS)_3$. **d**. methylated version of **c**. **e**. Endo H treated form of **d**. **f**. MV-H (residues Ser^{184} to Thr^{607})-maSLAM-V (residues Met^{30} to Gln^{140} with N102H/R108Y substitutions) fused by a 12-residue flexible linker $(GGGS)_3$. **g**. methylated version of **f**. **h**. MV-H (residues Ser^{184} to Thr^{607} with L482R substitution)-maSLAM-V (residues Met^{30} to Gln^{140} with N102H/R108Y substitutions) protein conjugated by a 12-residue flexible linker $(GGGS)_3$. **i**. methylated version of **h**. The mark "-" in the resolution column indicates that no crystals were obtained.

crystals were obtained, and diffraction was improved from 7-8 Å to 4.5 Å. Therefore, chemical modification has a potential to improve the crystallization, leading to diffraction-quality crystals.

Because both maSLAM and hSLAM V domain proteins were expressed poorly (only ~100 μg per 1L cell culture medium), only limited numbers of crystallization trials were possible. In addition, the slightly weak binding affinity between SLAMs and MV-H (*Kd* = ~0.4 μM) [13] would further impede formation of co-complex crystals. To solve these two problems, we inserted either the $(GGGS)_2$ or $(GGGS)_3$ linker between the C-terminus of MV-H (Ser^{184} to Thr^{607}) and the N-terminus of maSLAM (Met^{30} to Gln^{140}), resulting in the MV-H-$(GGGS)_n$ linker-maSLAM-V complex as a single chain construct. Notably, protein expressions were dramatically improved (~3 mg per 1L cell culture medium), with similar protein yields for both $(GGGS)_2$ and $(GGGS)_3$ linker constructs. These proteins were further lysine-methylated. Although the MV-H-$(GGGS)_3$ linker-hSLAM-V complex was also sufficiently obtained, it failed to crystallize. In initial screenings, crystals of MV-H-$(GGGS)_3$-maSLAM-V complex were obtained under a broader range of conditions than those of the complex with the $(GGGS)_2$ linker, and thus the $(GGGS)_3$ linker was used in subsequent protein preparations and crystallizations.

Next, the N102H substitution of maSLAM-V was carried out to remove an N-linked glycosylation site that appeared to interfere with crystal packing, as based on our preliminary low-resolution data (Supplementary Fig. (1A)). N102 is located on the crystallographic protein-protein interface comprised of BED sheets and loops from two SLAM-V domains. The crystals of the MV-H-maSLAM-V (with the N102H substitution) conjugated by a 12-residue flexible linker $(GGGS)_3$ were obtained with the ComPAS suite solution G9 (100 mM sodium acetate, pH 4.6, 1.0 M sodium formate). Prior to further optimization, the protein was treated using Endo H in reaction buffer (50 mM sodium acetate pH 5.4, 100 mM NaCl) at 310 K for 3h, and re-purified by size exclusion chromatography with buffer containing 20 mM imidazole, pH 8.0, and 100 mM NaCl. The crystals were grown

by the hanging drop vapor diffusion method at 293K from drops containing 1 ml each of protein solution (14.3 mg/ml, in 20 mM imidazole, pH 8.0, 100 mM NaCl) and mother liquor (100 mM imidazole, pH 7.0, 0.6 M sodium malonate, 2 % ethylene glycol) Fig. (**2B**). Crystals of the MV-H-maSLAM-V complex became suitable for cryo-experiment by increasing the concentration of ethylene glycol to 25 %. A diffraction data set was collected to 4.0 Å resolution at 100 K, from a single largest crystal, at beamline BL5A of Photon Factory in KEK (Tsukuba, Japan). Thus, the single-chain formation and Endoglycosidase H (Endo-H) treatment assisted the protein expression and diffraction, improving resolution from 4.5 Å to 4.0 Å.

R108 is also located on the same interface as N102 on SLAM-V domain. Due to crystallographic protein-protein packing, the two neighboring R108 residues might present steric repulsion. In CD48, a tyrosine is located at the corresponding 108 position. Therefore, an arginine to tyrosine substitution in maSLAM-V was carried out to facilitate hydrophobic interactions and better packing. Additional mutations at K93, R95, R97, S104 and A106, all of which are located at or close to crystal packing interface, did not improve resolutions even upon methylation (Supplementary Fig. (**1B,C**). The crystals of the MV-H-maSLAM-V (with N102H/R108Y substitutions) conjugated by a 12-residue flexible linker $(GGGS)_3$ were obtained with the Crystal Screen II solution No. 15 (100 mM sodium citrate tribasic dihydrate, pH 5.6, 1.0 M lithium sulfate monohydrate, 0.5 M Ammonium sulfate). Crystals were grown by floating-drop vapor diffusion at 293 K from drops containing 1 µl each of protein solution (10.0 mg/ml, in 20 mM imidazole, pH 8.0, 100 mM NaCl) and mother liquor (100 mM imidazole, pH 5.8, 0.7 M lithium sulfate monohydrate, 0.5 M Ammonium sulfate, 2 % ethylene glycol) Fig. (**2C**) [22]. Crystals of the MV-H-maSLAM-V (N102H/R108Y) complex became suitable for cryo-experiment by using 2.3 M lithium acetate together with mother liquor. A diffraction data set was collected to 3.55 Å resolution at 100 K, from a single largest crystal, at beamline BL41XU of SPring-8 (Harima, Japan). Crystals of the above three MV-H-SLAM complexes were also indexed to the same space group $P6_322$ and have similar unit cell dimensions. Due to this structure-guided mutation, the resolution improved from 4.0 Å to 3.55 Å.

Finally, the L482R substitution of MV-H was used to increase the stability of MV-H-SLAM complex, based on preliminary functional study (unpublished data). This L482R substitution is indeed found in a clinical isolate of MV (genotype D1 (Genbank, 80805)). The highest resolution crystal of the MV-H (with the L482R substitution)-maSLAM-V (with N102H/R108Y substitutions) conjugated by a 12-residue flexible linker $(GGGS)_3$ was grown by the floating-drop vapor diffusion method at 293 K from drop containing 1 µl each of protein solution (11.3 mg/ml, in 20 mM imidazole, pH 8.0, 100 mM NaCl) and mother liquor (0.1 M imidazole, pH 8.3, 0.7 M lithium sulfate monohydrate, 0.5 M Ammonium sulfate, 0.05 M lithium acetate) Fig. (**2D**). Crystals of the MV-H (L482R)-maSLAM-V (N102H/R108Y) complex were cryo-protected with mother liquid supplemented with 2.0 M lithium acetate. A single diffraction data set was collected to 3.15 Å resolution at 100 K at beamline BL5A of Photon Factory in KEK (Tsukuba, Japan). Floating-drop vapor diffusion method yield bigger crystals than the hang-drop vapor diffusion method and was subsequently used for further experiments Fig. (**3**). The L482R mutation allowed for an additional 0.4 Å improvement to a final resolution of 3.15 Å.

PHASE DETERMINATION

Phases were determined by molecular replacement using a previously reported structure of the MV-H head domain (PDB ID: 2ZB6) [13] as a search model in Phaser (ccp4 suite) [23]. Resulting electron-density map allowed tracing of the main chain polypeptides. Structure of SLAM was determined by manual model fitting based on the structure of

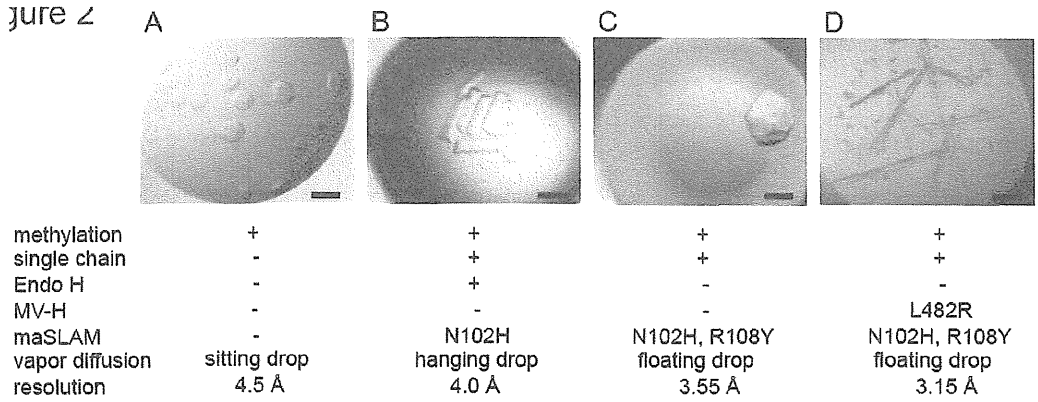

Figure 2. Crystals of MV-H-maSLAM-V complex. A, Crystals of 1:1 complex of methylated MV-H (residues Asp^{149} to Arg^{617}) and SLAM (residues Met^{1} to Gln^{140}) proteins produced by sitting-drop vapor diffusion at 293 K. **B**, Crystals of MV-H (residues Ser^{184} to Thr^{607})-maSLAM-V (residues Met^{30} to Gln^{140} with N102H substitution) protein linked by a 12-residue flexible linker $(GGGS)_3$, which was treated by Endo H and methylated, and produced by hanging-drop vapor diffusion at 293 K. **C**, Crystals of methylated MV-H-maSLAM-V (with N102H/R108Y substitutions) complex protein produced by floating-drop vapor diffusion at 293 K. **D**, Crystals of methylated MV-H (with the L482R substitution)-maSLAM-V (with N102H/R108Y substitutions) protein produced by floating-drop vapor diffusion at 293 K. All proteins were expressed in HEK293SGnTI(-) cells. Scale bars represent 0.3 mm.

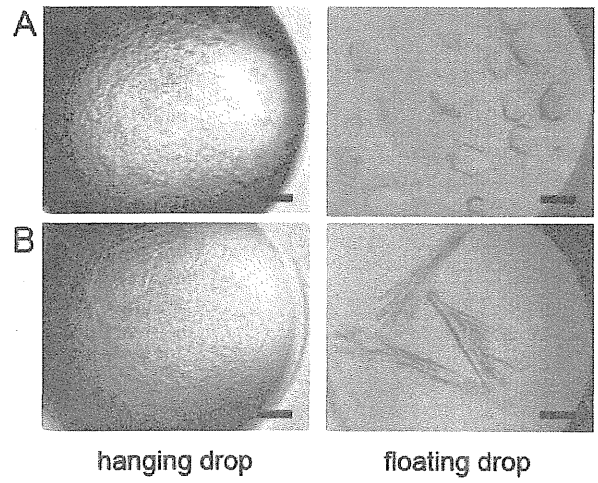

Figure 3. Hanging- and floating-drop vapor diffusions. The left and right panels show crystals grown by hanging-drop vapor and floating-drop vapor diffusion, respectively. **A**, Crystals of methylated MV-H-maSLAM-V (with N102H/R108Y substitutions) complex as described in Fig. (**2C**). **B**, Crystals of methylated MV-H (with the L482R substitution)-maSLAM-V (with N102H/R108Y substitutions) protein as described in Figure 2D. Scale bars represent 0.3 mm.

CD48. Subsequent model building and structure refinement were carried out with Phenix [24] and Refmac [25], coupled with the model correction function of Lafirein [26]. Iterative manual model building and correction were done using COOT [27]. The final structure was refined to R and R_{free} factors of 23.1 % and 29.2 %, respectively. The difference between refinement R and R_{free} is relatively high. One of the reasons is that the N-terminal and C-terminal regions of bound SLAM molecule have only poor electron density for the four molecules in an asymmetric unit. However, the presence of an intra-disulfide bond in the SLAM molecule between Cys32-Cys132 definitely reveals the location of these regions. Furthermore, the data set of the 3.15 Å-diffracted crystal got some problems such as anisotropy, spot splits, and streaky spots. Additional crystallographic statistics are listed in **Supplementary Table 1**.

CONCLUSIONS

MV-H-SLAM complexes have been successfully crystallized after ~200 different plasmid constructs were examined. Improved diffraction was obtained by employing the following techniques; (1) a transient expression system in HEK293SGnTI(-) cells, (2) methylation of lysine, (3) substitution of amino acid residues based on available structural and functional information, (4) single-chain formation, (5) Endo-H treatment and (6) floating-drop vapor diffusion. Methylation of lysine and Endo-H treatment might have reduced the repulsion by electrostatic effect and steric hindrance by N-linked sugars, respectively. Single-chain formation likely allowed the complex to stabilize, resulting in the improvement of protein expression. Substitutions of amino acid residues might also have helped crystallization by reducing the repulsion and steric hindrance. In general, weak protein-protein interaction would impede crystallization efforts. Hence, these engineering methods presented in this study, used individually or in combination, would be useful for improving crystallization of the protein complexes between a variety of glycoproteins and their receptors.

ACKNOWLEDGEMENTS

We thank the beam-line staff of Photon Factory (Tsukuba, Japan) and SPring8 (Hyogo, Japan) for technical help during data collection. We also thank M. A. Billeter (Institute of Molecular Biology, University of Zurich) for reagents, M. Takeda, I. Tanaka, K. Inaba, K. Mihara, T. Oka, H. Aramaki, K. Tokunaga, M. Kajikawa, K. Kuroki and K. Sasaki for discussion, and Adrianna P.P. Zhang for reviewing the manuscript. This work was supported by grants from the Ministry of Education, Culture, Sports, Science and Technology and the Ministry of Health, Labor and Welfare of Japan. T. H. is supported by JSPS Research Fellowship for Young Scientists.

SUPPLEMENTARY MATERIAL

Supplementary Material is available on Protein & Peptide Letters website.

REFERENCES

[1] Lamb, R. A.; Parks, G. D., Paranyxiviridae: The Viruses and Their Replication. In: Fields Virology, 5th edn; D. M. Knipe, P. M. H., D. E. Griffin, R. A. Lamb, M. A. Martin, B. Roizman & S. E. Straus. , Ed. Lippincott Williams & Wilkins.: Philadelphia, 2007; pp 1449-1496.

[2] Bryce, J.; Boschi-Pinto, C.; Shibuya, K.; Black, R. E., WHO estimates of the causes of death in children. *Lancet,* **2005**, *365* (9465), 1147-52.

[3] Griffin, D. E., Measles Virus. In: Fields Virology, 5th edn; D. M. Knipe, P. M. H., D. E. Griffin, R. A. Lamb, M. A. Martin, B. Roizman & S. E. Straus. , Ed. Lippincott Williams & Wilkins.: Philadelphia, 2007; pp 1551-1585.

[4] Yanagi, Y.; Takeda, M.; Ohno, S.; Hashiguchi, T., Measles virus receptors. *Curr. Top. Microbiol. Immunol.,* **2009**, *329*, 13-30.

[5] Cocks, B. G.; Chang, C.-C. J.; Carballido, J. M.; Yssel, H.; de Vries, J. E.; Aversa, G., A novel receptor involved in T-cell activation. *Nature,* **1995**, *376*, 260-263.

[6] Kiel, M. J.; Yilmaz, O. H.; Iwashita, T.; Yilmaz, O. H.; Terhorst, C.; Morrison, S. J., SLAM family receptors distinguish hematopoietic stem and progenitor cells and reveal endothelial niches for stem cells. *Cell,* **2005**, *121* (7), 1109-21.

[7] Tatsuo, H.; Ono, N.; Tanaka, K.; Yanagi, Y. SLAM (CDw150) is a cellular receptor for measles virus. *Nature,* **2000**, *406*, 893-897.

[8] Noyce, R. S.: Bondre, D. G.: Ha, M. N.: Lin, L. T.: Sisson, G.: Tsao, M. S.: Richardson, C. D. Tumor cell marker PVRL4 (nectin 4) is an epithelial cell receptor for measles virus. *PLoS Pathog.,* **2011**, *7*(8): e1002240.

[9] Mühlebach, M. D.: Mateo, M.: Sinn, P. L.: Prüfer, S.: Uhlig, K. M.: Leonard, V. H.: Navaratnarajah, C. K.: Frenzke, M.: Wong, X. X.: Sawatsky, B.: Ramachandran, S.: McCray, P. B. Jr.: Cichutek, K.: von Messling, V.: Lopez, M.: Cattaneo, R. Adherens junction protein nectin-4 is the epithelial receptor for measles virus. *Nature,* **2011**, *480*(7378), 530-533.

[10] (a) Takeda, M.; Tahara, M.; Hashiguchi, T.; Sato, T. A.; Jinnouchi, F.; Ueki, S.; Ohno, S.; Yanagi, Y., A human lung carcinoma cell line supports efficient measles virus growth and syncytium formation via a SLAM- and CD46-independent mechanism. *J. Virol.,* **2007**, *81* (21), 12091-6; (b) Tahara, M.; Takeda, M.; Shirogane, Y.; Hashiguchi, T.; Ohno, S.; Yanagi, Y., Measles virus infects both polarized epithelial and immune cells by using distinctive receptor-binding sites on its hemagglutinin. *J. Virol.,* **2008**, *82* (9), 4630-7.

[11] Leonard, V. H.; Sinn, P. L.; Hodge, G.; Miest, T.; Devaux, P.; Oezguen, N.; Braun, W.; McCray, P. B., Jr.; McChesney, M. B.; Cattaneo, R., Measles virus blind to its epithelial cell receptor remains virulent in rhesus monkeys but cannot cross the airway epithelium and is not shed. *J. Clin. Invest.,* **2008**, *118* (7), 2448-58.

[12] Santiago, C.; Celma, M. L.; Stehle, T.; Casasnovas, J. M., Structure of the measles virus hemagglutinin bound to the CD46 receptor. *Nat. Struct. Mol. Biol.,* **2010**, *17* (1), 124-9.

[13] Hashiguchi, T.; Kajikawa, M.; Maita, N.; Takeda, M.; Kuroki, K.; Sasaki, K.; Kohda, D.; Yanagi, Y.; Maenaka, K., Crystal structure of measles virus hemagglutinin provides insight into effective vaccines. *Proc. Natl. Acad. Sci. USA,* **2007**, *104* (49), 19535-40.

[14] Hashiguchi, T.; Ose, T.; Kubota, M.; Maita, N.; Kamishikiryo, J.; Maenaka, K.; Yanagi, Y., Structure of the measles virus hemagglutinin bound to its cellular receptor SLAM. *Nat. Struct. Mol. Biol.,* **2011**.

[15] Colf, L. A.; Juo, Z. S.; Garcia, K. C., Structure of the measles virus hemagglutinin. *Nat. Struct. Mol. Biol.,* **2007**, *14* (12), 1227-8.

[16] Ono, N.; Tatsuo, H.; Tanaka, K.; Minagawa, H.; Yanagi, Y., V domain of human SLAM (CDw150) is essential for its function as a measles virus receptor. *J. Virol.,* **2001**, *75*, 1594-1600.

[17] Reeves, P. J.; Callewaert, N.; Contreras, R.; Khorana, H. G., Structure and function in rhodopsin: high-level expression of rhodopsin with restricted and homogeneous N-glycosylation by a tetracycline-inducible N-acetylglucosaminyltransferase I-negative HEK293S stable mammalian cell line. *Proc. Natl. Acad. Sci. USA,* **2002**, *99* (21), 13419-24.

[18] Hashiguchi, T.; Kajikawa, M.; Maita, N.; Takeda, M.; Kuroki, K.; Sasaki, K.; Kohda, D.; Yanagi, Y.; Maenaka, K., Homogeneous sugar modification improves crystallization of measles virus hemagglutinin. *J. Virol. Methods,* **2008**, *149* (1), 171-4.

[19] Rayment, I.; Rypniewski, W. R.; Schmidt-Base, K.; Smith, R.; Tomchick, D. R.; Benning, M. M.; Winkelmann, D. A.; Wesenberg, G.; Holden, H. M., Three-dimensional structure of myosin subfragment-1: a molecular motor. *Science,* **1993**, *261* (5117), 50-8.

[20] Otwinowski, Z.; Minor, W., Processing of X-ray Diffraction Data Collected in Oscillation Mode. *Methods Enzymol.,* **1997**, *276*, 307-326.

[21] Walter, T. S.; Meier, C.; Assenberg, R.; Au, K. F.; Ren, J.; Verma, A.; Nettleship, J. E.; Owens, R. J.; Stuart, D. I.; Grimes, J. M., Lysine methylation as a routine rescue strategy for protein crystallization. *Structure,* **2006**, *14* (11), 1617-22.

[22] Adachi, H.; Takano, K.; Morikawa, M.; Kanaya, S.; Yoshimura, M.; Mori, Y.; Sasaki, T., Application of a two-liquid system to sitting-drop vapour-diffusion protein crystallization. *Acta Crystallogr. D. Biol. Crystallogr.,* **2003**, *59* (Pt 1), 194-6.

[23] McCoy, A. J.; Grosse-Kunstleve, R. W.; Adams, P. D.; Winn, M. D.; Storoni, L. C.; Read, R. J., Phaser crystallographic software. *J. Appl. Crystallogr.,* **2007**, *40* (Pt 4), 658-674.

[24] Adams, P. D.; Afonine, P. V.; Bunkoczi, G.; Chen, V. B.; Davis, I. W.; Echols, N.; Headd, J. J.; Hung, L. W.; Kapral, G. J.; Grosse-Kunstleve, R. W.; McCoy, A. J.; Moriarty, N. W.; Oeffner, R.; Read, R. J.; Richardson, D. C.; Richardson, J. S.; Terwilliger, T. C.; Zwart, P. H., PHENIX: a comprehensive Python-based system for macromolecular structure solution. *Acta Crystallogr. D. Biol. Crystallogr.,* **2010**, *66* (Pt 2), 213-21.

[25] Murshudov, G. N.; Vagin, A. A.; Dodson, E. J., Refinement of macromolecular structures by the maximum-likelihood method. *Acta Crystallogr. D. Biol. Crystallogr.,* **1997**, *53* (Pt 3), 240-55.

[26] Yao, M.; Zhou, Y.; Tanaka, I., LAFIRE: software for automating the refinement process of protein-structure analysis. *Acta Crystallogr. D. Biol. Crystallogr.,* **2006**, *62* (Pt 2), 189-96.

[27] Emsley, P.; Cowtan, K., Coot: model-building tools for molecular graphics. *Acta Crystallogr. D. Biol. Crystallogr.,* **2004**, *60* (Pt 12 Pt 1), 2126-32.

Received: May 17, 2011 Revised: August 18, 2011 Accepted: August 20, 2011

JCM
Journals.ASM.org

No Evidence for an Association between Persistent Measles Virus Infection and Otosclerosis among Patients with Otosclerosis in Japan

Noritaka Komune,[a,b] Mitsuru Ohashi,[b] Nozomu Matsumoto,[b] Takashi Kimitsuki,[b] Shizuo Komune,[b] and Yusuke Yanagi[a]

Departments of Virology[a] and Otorhinolaryngology,[b] Faculty of Medicine, Kyushu University, Higashi-ku, Fukuoka, Japan

Otosclerosis, which is characterized by disordered bone remodeling, occurs exclusively in the human temporal bone. The etiology of the disease is unknown, but a popular hypothesis is that it is caused by persistent measles virus (MV) infection. Paramyxovirus-like filamentous structures were found in otosclerotic lesions of stapes footplates from patients with otosclerosis. Although MV RNAs have been detected in otosclerotic samples by using reverse transcription-PCR, no complete MV mRNA sequence has been reported, nor has infectious virus been isolated from clinical samples. Furthermore, one study failed to obtain evidence of MV infection in otosclerotic bone samples. In this study, we tested, by three different protocols, for the presence of MV in clinical samples from patients with otosclerosis in Japan. We used a highly sensitive reverse transcription-quantitative PCR method which is able to detect viral mRNA in cells infected with MV at around one infectious unit per well. We obtained no evidence of MV infection in bone samples, primary cell cultures derived from stapes bones, or MV-susceptible cell lines (Vero/hSLAM and II-18 cells) cocultured with bone samples or primary cell cultures derived from them. Thus, our results do not support the hypothesis that persistent MV infection is involved in the pathoetiology of otosclerosis.

Antonio Maria Valsalva, an Italian anatomist and surgeon, first reported a lesion of otosclerosis in a dissected temporal bone from a patient with hearing impairment (18). Otosclerosis is characterized by disordered bone remodeling in the otic capsule. The disease is thought to start in an area anterior to the stapes footplate and the oval window niche called the fissula ante fenestram, as often observed by computed tomography (CT). In most cases, the stapes bone becomes fixed due to invasion of otosclerotic foci at the stapediovestibular joint. This fixation results in conductive hearing loss, which is often accompanied by Carhart's notch (2-kHz bone conduction threshold dip) and negative stapedius reflex with the normal tympanic membrane. In advanced stages, otosclerosis foci can involve the cochlea and the vestibule, leading to sensorineural hearing loss and vertigo, respectively, and pathological involvement of the anterior and/or posterior pole can be observed. Otosclerosis occurs at a prevalence of 0.04 to 1% among Caucasian people (18), whereas it is uncommon among Asians and extremely rare among Africans. Recently, the incidence of otosclerosis has been increasing in Japan (44).

This disorder of bone turnover that leads to abnormal resorption and redeposition of the bone is similar to the lesion observed in Paget's disease (PD), which has been proposed to be a chronic inflammatory disease caused by persistent measles virus (MV) infection. Although the pathogenesis of otosclerosis remains unknown, many hypotheses, including autoimmune response, viral infection, endocrine disorder, connective tissue disorder, and genetic disease (5), have been proposed. One of the most suspected environmental factors is persistent MV infection, like for PD.

Measles is an acute febrile infectious disease which remains a major cause of child deaths in developing countries. MV, a member of the *Morbillivirus* genus in the *Paramyxoviridae* family, is an enveloped virus with a nonsegmented negative-strand RNA genome. The MV genome has six genes that encode the nucleocapsid (N), phospho (P), matrix (M), fusion (F), hemagglutinin (H), and large (L) proteins. MV is serologically monotypic, but based on the sequences of the N and H genes, wild-type viruses are classified into eight clades designated A, B, C, D, E, F, G, and H. The Edmonston strain, the first MV isolate (6), is classified as genotype A and has been used in many studies, including for the development of vaccines.

The observation of filamentous structures morphologically similar to viral nucleocapsids in the endoplasmic reticulum (ER) of osteoblast-like cells of otosclerotic lesions led McKenna et al. to propose that otosclerosis might be caused by a viral infection (22). Since then, a number of studies have reported the detection of MV in samples from otosclerosis patients by using the reverse transcription-PCR (RT-PCR) method (4, 13, 14, 16, 17, 20, 26, 27) and immunohistochemical analysis (3, 21). Additionally, Arnold et al. analyzed the data for all patients who were hospitalized for otosclerosis in Germany from 1993 to 2004 (2). They concluded that there is a statistically significant decrease in otosclerosis among patients who were vaccinated against MV in comparison with the patients who were not vaccinated (2). Despite many studies that demonstrated the presence of MV in otosclerotic tissue, the complete MV mRNA sequence has never been reported, nor has the isolation of MV from otosclerotic samples been successful. Grayeli et al. reported that MV RNA was not detected in fresh otosclerotic samples in a large population of patients ($n = 35$) (9). The presence of different viruses was also reported in some cases (21, 37). Moreover, there is no evidence that infection of the otic capsule with MV produces cells with the otosclerotic phenotype in this tissue.

In this study, we tested for the presence of MV (gene and in-

Received 25 October 2011 Returned for modification 15 December 2011
Accepted 20 December 2011
Published ahead of print 28 December 2011
Address correspondence to Noritaka Komune, ks06025@virology.med.kyushu-u.ac.jp.

doi:10.1128/JCM.06163-11

TABLE 1 Clinical data for all patients

Sample no.[a]	Sample type	Diagnosis[b]	Side[c]	Sex[d]	Age (yr)	Bilateral/unilateral	Tympanic membrane	FAF[e]	CN[f]	Stapedius reflex	Tympanometry[g]	History of measles	Operative procedure
1-1 A	Fresh frozen	OS	R	F	65	Bilateral	Normal	+	+	+	A	+	Stapedectomy
1-2	Fresh frozen	OS	L	F	50	Unilateral	Normal	−	+	−	A	+	Stapedectomy
1-3 B	Fresh frozen	OS	R	F	63	Bilateral	Normal	−	−	−	A	Unknown	Stapedectomy
1-4	Fresh frozen	TS	R	F	65	Unilateral	Lateralization	−	−	NE[h]	NE	Unknown	Stapedectomy
1-5	Fresh	OS	R	F	50	Bilateral	Normal	+	+	−	A	Unknown	Stapedectomy
2-1	Fresh	OS	L	F	67	Bilateral	Normal	+	+	−	As	Unknown	Stapedotomy
2-2 C	Fresh	OS	L	F	58	Bilateral	Normal	−	+	−	A	+	Stapedotomy
2-3	Fresh	OS	L	F	66	Bilateral	Calcification	−	−	−	NE	+	Stapedectomy
2-4	Fresh	OS	R	F	56	Bilateral	Normal	+	−	NE	As	Unknown	Stapedectomy
2-5 D	Fresh	OS	R	M	37	Bilateral	Normal	−	−	NE	A	Vaccinated	Stapedectomy
2-6 A	Fresh	OS	L	F	66	Bilateral	Normal	+	+	−	A	+	Stapedectomy
2-7	Fresh	OS	L	F	46	Bilateral	Normal	+	−	−	As	Unknown	Stapedectomy
2-8	Fresh	Chole	R	M	64	Unilateral	Postoperative state	−	+	NE	NE	Unknown	Stapedectomy
2-9	Fresh	OS	R	F	56	Unilateral	Normal	−	+	−	A	+	Stapedectomy
2-10 E	Fresh	OS	R	F	50	Bilateral	Normal	+	−	−	As	+	Stapedotomy
2-11	Fresh	OS	R	F	50	Bilateral	Normal	+	+	−	A	Unknown	Stapedectomy
3-1	Fresh frozen	OS	L	F	49	Bilateral	Normal	+	−	−	A	+	Stapedectomy
3-2	Fresh frozen	OS	R	M	57	Bilateral	Normal	+	+	NE	A	Unknown	Stapedectomy
3-3	Frozen in TRIzol	OS	L	F	46	Bilateral	Scar	−	+	−	A	+	Stapedectomy
3-4	Frozen in TRIzol	OS	L	M	25	Bilateral	Normal	−	−	−	As	+	Stapedectomy
3-5	Frozen in TRIzol	OS	L	M	23	Unilateral	Slightly retracted	−	−	−	A	Vaccinated	Stapedectomy
3-6 B	Frozen in TRIzol	OS	L	F	65	Bilateral	Normal	−	−	−	As	Unknown	Stapedectomy
3-7 D	Frozen in TRIzol	OS	L	M	38	Bilateral	Normal	−	−	NE	A	Vaccinated	Stapedectomy
3-8 C	Frozen in TRIzol	OS	R	F	60	Bilateral	dull	−	+	+	A	+	Stapedotomy
3-9 E	Frozen in TRIzol	OS	L	F	51	Bilateral	Normal	+	−	−	As	+	Stapedotomy
3-10	Frozen in TRIzol	OS	R	F	67	Bilateral	Postoperative state	−	+	−	As	+	Stapedectomy
3-11	Frozen in TRIzol	OS	L	F	56	Unilateral	Normal	−	+	−	As	Unknown	Stapedectomy

[a] Samples from the same patient are marked with the same letter.
[b] OS, otosclerosis; TS, tympanosclerosis; Chole, cholesteatoma.
[c] R, right; L, left.
[d] F, female; M, male.
[e] FAF, low density at fissula ante fenestram in computed tomography.
[f] CN, Carhart's notch in pure-tone audiometry.
[g] A, normal; As, ossicular fixation, tympanosclerosis, or otitis media with effusion.
[h] NE, not examined.

fectious virus) in stapes bones from patients with otosclerosis in Japan using highly sensitive detection methods.

MATERIALS AND METHODS

Patients. The clinical data for all patients, which were obtained from medical files, are given in Table 1. There were 5 male patients (6 ears) and 17 female patients (21 ears). The mean age was 51.05 years (range, 23 to 67). Preoperative vestibular symptoms such as vertigo were not reported in any cases. Preoperative diagnosis was made by clinical course and examinations of pure tone audiometry (PTA), stapedius reflexes (SR), tympanometry, and CT of the temporal bone. The grade of otosclerosis was considered to be extensive (with associated sensorineural hearing loss) in 17 ears. The definitive diagnosis of otosclerosis was made during surgery by the condition of the stapes bones and their immobility. All patients showed fixation of the stapes bone. During surgery, the involved stapes bones were removed. The removal of the whole stapes bone, called a stapedectomy, was performed in 22 cases (81%). The removal of its superstructure, called a stapedotomy, was performed in 5 cases (19%). Approval by the ethics committee of Kyusyu University Hospital and the patient consent were obtained for these samplings and all experimental procedures.

Cells and viruses. The characteristics and culture conditions of the Vero/hSLAM (33) and II-18 (38) cell lines were as described previously. The MV used in this study was a recombinant virus, based on the wild-type IC-B strain, expressing enhanced green fluorescent protein (IC323-EGFP) (10). The virus was grown on Vero/hSLAM cells, and virus titers were determined by plaque assay on Vero/hSLAM cells. cDNAs prepared from MV isolates of genotypes D3, D4, D5 (two stocks isolated in 2000 and 2008), D8, D9, G3, and H1, were kindly provided by Y. Nakatsu, K. Komase, and M. Takeda (National Institute of Infectious Diseases, Tokyo, Japan). These cDNAs were synthesized from RNAs directly extracted from virus stocks using a viral RNA minikit (Qiagen). A mixture of random hexamers was used for cDNA synthesis.

Reverse transcription-quantitative PCR (RT-QPCR). Total RNA was extracted from bone samples using TRIzol (Life Technologies) and chloroform (1:0.2, vol/vol) and precipitated with isopropanol. Primary cells and cocultured cells were lysed with the lysis buffer from the Agilent total RNA isolation minikit (Agilent), and total RNA was then isolated according to the manufacturer's instructions. The extracted RNAs were treated with RQ1 DNase (Promega) and reverse transcribed into cDNAs using SuperScript III reverse transcriptase (Invitrogen Life Technologies) and random hexamers. PCR (70 cycles of 95°C for 5 s and 60°C for 20 s) was then performed with SYBR Premix Ex *Taq* II (TaKaRa Bio Inc.) in capillary tubes. Fluorescence of SYBR green was monitored at the end of each PCR cycle with a LightCycler instrument (Roche Diagnostics, Indianapolis, IN). cDNAs for the β-actin and viral N mRNAs were amplified with actin-f/actin-r and N-f/N-r primer pairs as described previously (24, 40). The amplified products were separated by electrophoresis on 1.5% or 3% agarose gels containing ethidium bromide and were visualized by UV light.

Plasmids. p(+)MV323-EGFP encodes the full-length antigenomic cDNA of the virulent IC-B strain of MV (10). pGEM-T-actin was generated by inserting a DNA fragment encoding actin into the expression vector pGEM-T. The copy numbers of these plasmids were calculated, and they were used as positive controls in the QPCR assay. cDNA derived from the genome of the Edmonston tag strain (31, 34) was also used in the experiment that assessed the sensitivity of the N-f/N-r primer pair.

Analysis of clinical samples. In the first protocol, stapes bone fragments were cocultured with 90% confluent Vero/hSLAM or II-18 cells in a 10-cm dish and observed for 7 to 12 days by light microscopy to check whether cytopathic effects (CPE) such as syncytium formation occurred. The presence of MV RNA in cocultured cells was examined by RT-QPCR. In the second protocol, fresh stapes bone fragments were placed in a 6-cm culture plate in McCoy's 5A medium (Invitrogen, Karlsruhe, Germany) supplemented with 20% fetal bovine serum (FBS), penicillin (100 U/ml), and streptomycin (100 μg/ml), as previously reported (8). After 3 to 4 weeks of incubation, primary cells migrated out of bone samples and reached maximal cellular growth. At this point, the primary cells were trypsinized, and stapes bones were used for RNA extraction. These primary cells were then cocultured with 60% confluent Vero/hSLAM or II-18 cells in a 10-cm dish and observed for 3 to 5 weeks. Another portion of the primary cells was placed in a 6-cm cell culture dish and allowed to grow to confluence for 2 to 3 additional weeks, and total RNA was extracted. In the third protocol, bone fragments were pulverized and total RNA was extracted directly from bone fragments by using TRIzol reagent. The presence of MV RNA was analyzed using the RT-QPCR method.

TABLE 2 Comparison between clinical and histological diagnoses for patients who underwent stapes surgery at Kyushu University Hospital during 2003 to 2009

Clinical diagnosis (n)	No. male/ no. female	Mean age, yr (range)	No. (%) with histologically diagnosed otosclerosis
Otosclerosis (47)	7/40	41.1 (17–77)	47/47 (100)
Tympanosclerosis (4)	2/2	58.25 (54–63)	0/4 (0)

RESULTS

Comparison between clinical and histological diagnoses. We first examined whether stapes bones from patients with clinically diagnosed otosclerosis in our institute had the same diagnosis histologically, because samples of stapes bones from patients to be used in our study would be diagnosed only clinically. Clinical diagnosis was perfectly matched with histological diagnosis in patients who underwent surgery for stapedial fixation at Kyushu University Hospital during 2003 to 2009 (the period before our study was initiated) (Table 2).

High sensitivity of the RT-QPCR method. We examined the sensitivity of our RT-QPCR method for detection of MV RNA. Vero/hSLAM cells were infected with serially diluted MV (IC323-EGFP) at 1/4 PFU per well to 40 PFU per well, followed by medium replacement and addition of the fusion block peptide (100 μg/ml) (35) at 2 h after incubation to block the second-round infection by progeny viruses. After 36 h of incubation, infectious units (IU) were determined by counting EGFP-expressing cells, the number of which was consistent with the PFU inoculated (Fig. 1). Total RNA was extracted from the infected cells, followed by RT-QPCR. To detect viral RNA, we used a pair of primers against the N gene, which is known to be most abundantly expressed in MV-infected cells (12). Our RT-QPCR method could detect the N mRNA in RNA extracted from cells infected with IC323-EGFP even at less than 1 IU/well (Fig. 1).

Next, we examined whether the primer pair used could detect different MV genotypes. We prepared cDNAs from MV isolates of the D3, D4, D5 (two stocks isolated in 2000 and 2008), D8, D9, G3, and H1 genotypes. These were the prevailing MV genotypes in Japan during the period from 1999 to 2011. We also prepared cDNA from the IC-B (genotype D3, isolated in 1990 in Japan) and Edmonston (genotype A) strains. Our primer pair could efficiently amplify the N genes from all these MV strains and isolates (Fig. 2).

Analysis of otosclerosis samples. MV infects immune cells and polarized epithelial cells by using SLAM and nectin 4, respectively, as receptors (28, 41). Vaccine strains of MV can also use CD46 as a receptor (41). Vero/hSLAM cells express SLAM and CD46. The lung adenocarcinoma cell line II-18 expresses nectin 4